Electric Field Tuning of the Rashba Effect in the Polar Perovskite Structures

K. V. Shanavas* and S. Satpathy
Department of Physics, University of Missouri, Columbia, Missouri 65211, USA
(Received 27 June 2013; published 25 February 2014)

We show that the Rashba effect at the polar perovskite surfaces and interfaces can be tuned by manipulating the two-dimensional electron gas by an applied electric field, using it to draw the two-dimensional electron gas out to the surface or push it deeper into the bulk, thereby controlling the surface-sensitive phenomenon. These ideas are illustrated by a comprehensive density-functional study of the recently discovered polar $KTaO_3$ surface. Analytical results obtained with a tight-binding model unravel the interplay between the various factors affecting the Rashba effect such as the strengths of the spin-orbit interaction and the surface-induced asymmetry. Our work helps interpret the recent experiments on the $KTaO_3$ surface as well as the $SrTiO_3/LaAlO_3$ interface.

DOI: 10.1103/PhysRevLett.112.086802 PACS numbers: 73.20.-r, 31.15.A-, 71.70.Ej

The Rashba effect describes the momentum-dependent spin splitting of the electron states at a surface or interface and is the combined result of the spin-orbit interaction (SOI) and the inversion-symmetry breaking [1]. It is commonly described by the Hamiltonian

$$\mathcal{H}_R = \alpha_R(\vec{k} \times \vec{\sigma}) \cdot \hat{z}, \tag{1}$$

where $\vec{k}$ is the electron momentum, $\vec{\sigma}$ its spin, and $\hat{z}$ is along the surface normal, which leads to a linear spin splitting in the band structure, $\varepsilon_k = (\hbar^2 k^2/2m) \pm \alpha_R k$. The Rashba coefficient α_R is proportional to the electric field for free electrons, but has a more complex dependence for electrons in the solid.

The control of the Rashba effect by an applied electric field in the solid is at the heart of a class of proposed spintronics devices for manipulating the electron spin [2]. This has been well studied for the hosted by the semiconductor quantum wells [3]. Recently, it has been shown that the 2DEGs hosted in the perovskite heterostructures [4,5] have many unusual properties leading to their potential applications in future devices with functionalities beyond what is known today. The perovskite interfaces are expected to have a much larger Rashba effect than their semiconductor counterparts, owing to the presence of high Z elements and a strongly localized two dimensional electron gas (2DEG) formed by the polar catastrophe. In fact, a strong Rashba effect was recently observed in the $LaAlO_3/SrTiO_3$ interface [6,7], which also showed an ill-understood asymmetric dependence on the sign of the electric field applied along the interface normal, while ordinarily one expects the magnitude of the Rashba effect to be independent of the field direction.

In this Letter, we show that the polar perovskite structures constitute an excellent system for the field control of the Rashba effect, aided by the relative ease with which the 2DEG can be manipulated in these polar structures. Detailed density-functional results are presented for the $KTaO_3$ (KTO) surface to illustrate the ideas.

2DEG at the KTO surface.—This surface is an ideal system for the study of the Rashba effect because Ta is a high Z element with strong SOI, a polar-catastrophe induced 2DEG has been observed there recently [8,9] similar to the LAO/STO interface, and, finally, a surface rather than an interface is more easily amenable to external electric fields. Figure 1 shows the basic features of the 2DEG formed at the KTO surface obtained from our

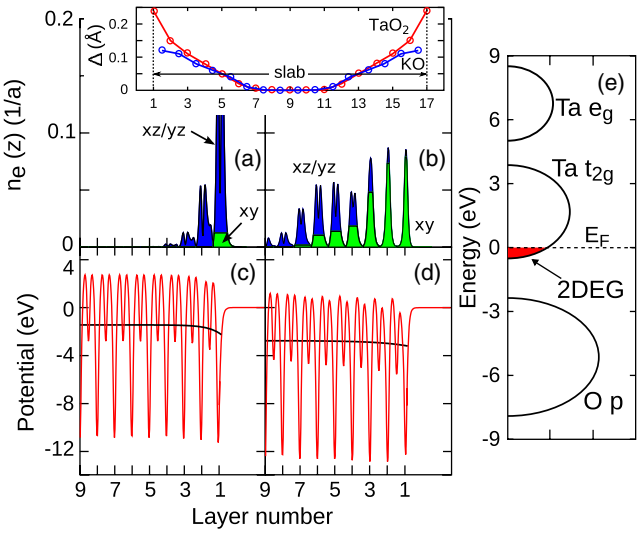

FIG. 1 (color online). Summary of the density-functional results for the $KTaO_3$ surface. The rightmost panel (e) shows the schematic band structure and the formation of the Ta t_{2g}-derived 2DEG at the surface. Panels (a) and (c) show the layer density profile of the 2DEG and the surface potential for the unrelaxed structure, while (b) and (d) show the same for the relaxed case. The topmost part shows the change of the cation-anion distances Δ in various layers due to relaxation, with layers No. 1 and 17 being the two surface Ta layers.

calculations using density-functional theory (DFT), performed with the generalized gradient approximation functional and the projector augmented wave pseudopotential method as implemented in the Vienna *ab initio* simulation package [10,11].

To simulate the TaO_2-terminated surface, we used a slab geometry consisting of 17 TaO_2 and 16 KO alternating layers corresponding to the formula unit $(KTO)_{16.5}$ and 24 Å of vacuum. We studied the Rashba effect by applying a series of electric fields and by fully relaxing the crystal structure in each case [12].

For the KTO surface, the alternating charged layers, nominally $(TaO_2)^{+1}$ and $(KO)^{-1}$, lead to the polar catastrophe just like in LAO/STO and as a result a 2DEG forms in the surface region terminated by TaO_2. Considerable structural relaxation, as expected for a polar surface, spreads the 2DEG several layers into the bulk. The relaxations, which produce local dipole moments screening out the surface polar field, decay rapidly within about six KTO layers and beyond that, the ionic positions return to their bulk values. A similar polar catastrophe argument leads to a two-dimensional hole gas for the ideal (defect free) KO-terminated surface; however, the Rashba effect is much smaller there [12].

Origin of the Rashba effect.—The microscopic origin of the Rashba effect is the relativistic SOI, $\mathcal{H}_{SO} = (\hbar^2/2m^2c^2)(\vec{\nabla}V \times \vec{k})\cdot\vec{\sigma}$, where $\vec{\nabla}V$ is the potential gradient. For a spherically symmetric potential, such as the field from a nucleus, it assumes the familiar form: $\mathcal{H}_{SO} = (m^2c^2r)^{-1}(\partial V/\partial r)\vec{L}\cdot\vec{S} = \xi\vec{L}\cdot\vec{S}$. In the presence of a symmetry-breaking surface electric field $E\hat{z}$, the first expression for $\mathcal{H}_{SO}$ leads to Eq. (1), with the Rashba coefficient $\alpha_R = -(\hbar^2 E/2m^2c^2)$. However, this coefficient is severely underestimated in the solids, if one naively identifies the electric field with the surface potential gradient.

Rather, the correct picture is that the Rashba SOI originates in the nuclear region due to the large nuclear field gradient there [13]. The second ingredient for the Rashba splitting is the electric-field induced hopping matrix elements, which diminish rapidly owing to the reduction of the strength of the broken inversion symmetry as one goes into the bulk [12] .We illustrate the net effect in Fig. 2 by computing the various contributions to the Rashba splitting for the Γ_6 bands in Fig. 3(a). We have isolated these contributions by keeping the SOI ξ either (i) on atoms in specific layers or (ii) on all atoms but within a specified spherical nuclear region and then by performing a single iteration with the self-consistent DFT potential obtained with all interactions present. As Fig. 2 shows, the dominant contribution comes from the nuclear region of atoms located in the first few surface layers. This in turn suggests the tuning of the Rashba effect by an electric field by moving the 2DEG in and out of the surface layers.

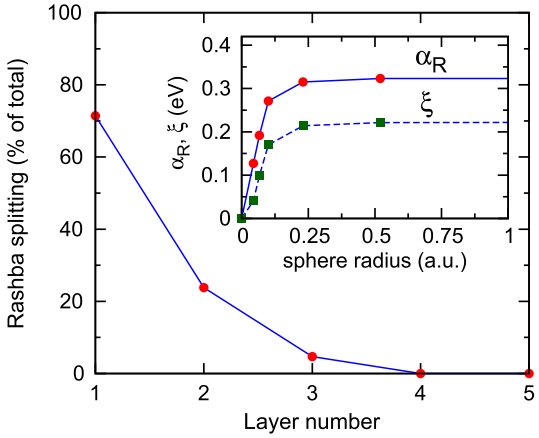

FIG. 2 (color online). Contribution from the various surface layers to the Rashba splitting of the lowest band in Fig. 3(a). Inset shows the Rashba coefficient α_R as well as the SOI parameter ξ as a function of the Ta sphere radius within which the nuclear electric field term $r^{-1}\partial V/\partial r$ was retained.

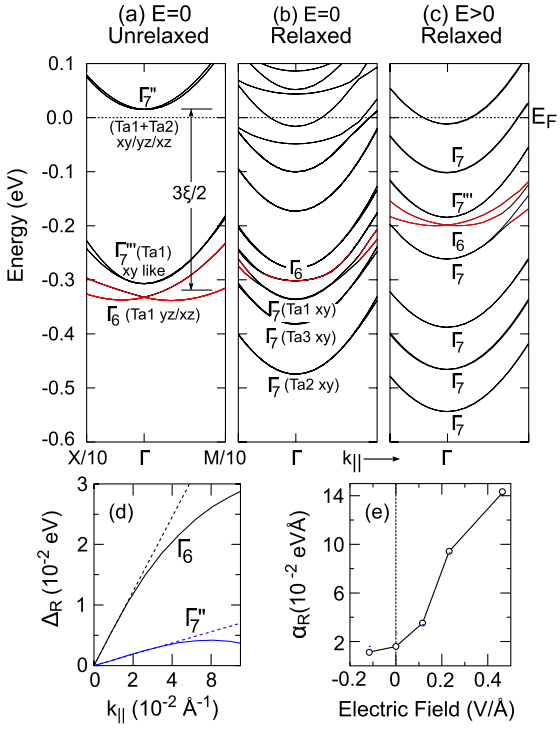

FIG. 3 (color online). Effect of surface relaxation and the applied electric field on the Rashba splitting for the KTO surface as obtained from DFT. Bands with strong Rashba splitting are shown in red. Relaxation causes the 2DEG to migrate deeper into the bulk diminishing the Rashba splitting (b), while an applied electric field ($E = 0.5$ V/Å) draws it back to the surface enhancing the splitting (c). (d) The splitting Δ_R as a function of $k_\parallel$ for bands in (a), the slopes of which yield $\alpha_R = 0.3$ eV·Å for Γ_6 and 0.05 eV·Å for Γ_7''. (e) The change of α_R with the applied electric field (positive E points into the bulk). The k points correspond to $X = (1, 0)$ and $M = (1, 1)$ in units of $2\pi a^{-1} = 2.56$ Å^{-1}.

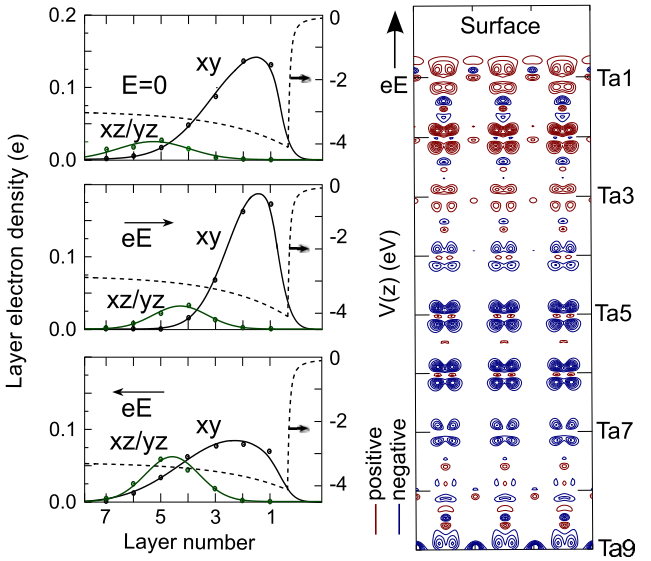

FIG. 4 (color online). the left side shows the layer density profile of the 2DEG (solid dots) with and without an applied electric field ($E = 0.12$ V/Å) calculated from DFT. The dashed lines indicate the cell-averaged potentials, while the solid lines are guides to the eye, with the black lines also indicating the electron leakage out of the surface obtained from solving the 1D Schrödinger equation with the surface potential. The right panel shows contours of the electron density change due to the applied electric field, which drives the electrons to the surface.

Electric field tuning.—We have calculated the Rashba splitting for the KTO surface by applying a series of electric fields. As seen from Fig. (3), the unrelaxed surface with zero field shows a very strong linear-k Rashba splitting because the 2DEG is sharply localized at the surface due to the strong polar field, extending to just three TaO_2 layers (Fig. 1). Relaxation of the surface atoms screens out the polar field and as a result, the 2DEG spreads deeper into the bulk region, thereby significantly diminishing the Rashba effect. This explains why in the ARPES experiments [8,9] on KTO, the Rashba splitting has not been seen despite the presence of a large spin-orbit coupling. On the contrary, application of an electric field draws the 2DEG towards the surface (Fig. 4), restoring back the Rashba effect. An electric field in the opposite direction drives the 2DEG deeper into the bulk and the Rashba splitting quickly becomes very small as the 2DEG is no longer present in the first few layers where the Rashba effect originates (see Fig. 2). Thus, we have demonstrated the field tuning of the Rashba effect as well as the very interesting asymmetric dependence on the direction of the applied electric field [Fig. 3(e)]. Such an asymmetric dependence was recently observed in the LAO/STO interface [7]. Note that the asymmetry is not expected for a nonpolar surface such as Au or Ag and a symmetric Rashba effect has been predicted there [14], presumably because it is difficult to alter the spatial position of the electron state by the applied field, unlike for the 2DEG in a nonpolar material.

Tight-binding description.—The Rashba splitting differs widely within the d orbital manifold, which may be understood in terms of the tight-binding (TB) model [15] on the cubic lattice that includes the surface asymmetry and the electric field:

$$\mathcal{H} = \mathcal{H}_{ke} + \mathcal{H}_{\mathrm{SO}} + \mathcal{H}_E + V_{\mathrm{sf}}. \tag{2}$$

The kinetic energy part contains the standard V_σ and V_π hopping between the d orbitals and the crystal field energies: $\mathcal{H}_{ke} = \sum_{ip\sigma} \varepsilon_{ip} n_{ip\sigma} + \sum_{ip,jq;\sigma} V_{ij}^{pq} c_{ip\sigma}^\dagger c_{jq\sigma} + \mathrm{H.c.}$, where $ip\sigma$ denotes the site-orbital-spin index. The O_h cubic field splits the d states into e_g and t_{2g} states. With the SOI included, the sixfold degenerate t_{2g} states (including spin) split into a twofold Γ_7^+ and a fourfold Γ_8^+ state, while the e_g remains unsplit with Γ_8^+ symmetry. The surface reduces the cubic symmetry into C_{4v} with Γ_7^+ going into Γ_7, while the Γ_8^+ state splits into $\Gamma_6 + \Gamma_7$, both twofold degenerate [16]. Note that

TABLE I. Rashba coefficient α_R and the pseudospin partner functions for the d states. Energies of the spin-orbit split states appear in the parenthesis and a is the lattice constant. If the SOI ξ is strong, but the electric field (parametrized by α, β, γ) is *not* weak, the Γ_7''' and the Γ_6 states do not reduce to the Rashba form, but must be described by a 4×4 matrix [Eq. (3)], while the Γ_7'' has the same α_R as in case 2. Strong cubic field splitting $\Delta \gg \xi$ is assumed.

	Surface field (C_{4v})		Rashba coefficients
Cubic field (O_h)	Symmetry	Rashba pseudospin partner functions	α_R/a
$e_g\ \Gamma_8^+(\Delta)$	$\Gamma_6(\Delta+\delta)$	$z^2\uparrow,\ z^2\downarrow$	$-2\sqrt{3}\beta\xi/\Delta$
	$\Gamma_7(\Delta)$	$x^2-y^2\uparrow,\ \ x^2-y^2\downarrow$	$-2\gamma\xi/\Delta$
t_{2g} case 1. Weak SOI, $\xi \ll \lvert\varepsilon\rvert$			
$\Gamma_7^+\ (\xi)$	$\Gamma_7(-\varepsilon)$	$xy\uparrow,\ xy\downarrow$	$2\alpha\xi/\epsilon$
$\Gamma_8^+\ (-\xi/2)$	$\Gamma_7'(\xi/2)$	$(yz\downarrow + ixz\downarrow)/\sqrt{2},\ (yz\uparrow - ixz\uparrow)/\sqrt{2}$	$2\alpha\xi/\epsilon$
	$\Gamma_6(-\xi/2)$	$(yz\downarrow - ixz\downarrow)/\sqrt{2},\ (yz\uparrow + ixz\uparrow)/\sqrt{2}$	$2\sqrt{3}\beta\xi/\Delta$
t_{2g} case 2. Strong SOI, $\xi \gg \lvert\varepsilon\rvert$, weak electric field $\lvert\alpha\rvert \ll \lvert\varepsilon\rvert$			
$\Gamma_7^+\ (\xi)$	$\Gamma_7''(\xi-\varepsilon/3)$	$(xy\uparrow + yz\downarrow + ixz\downarrow)/\sqrt{3},\ (xy\downarrow - yz\uparrow + ixz\uparrow)/\sqrt{3}$	$-4\alpha/3$
$\Gamma_8^+\ (-\xi/2)$	$\Gamma_7'''(-(3\xi+4\varepsilon)/6)$	$(2xy\uparrow - yz\downarrow - ixz\downarrow)/\sqrt{6},\ (2xy\downarrow + yz\uparrow - ixz\uparrow)/\sqrt{6}$	$4\alpha/3$
	$\Gamma_6(-\xi/2)$	$(yz\downarrow - ixz\downarrow)/\sqrt{2},\ (yz\uparrow + ixz\uparrow)/\sqrt{2}$	$2\sqrt{3}\beta\xi/\Delta$

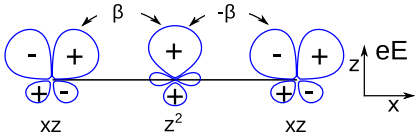

FIG. 5 (color online). Electric-field-induced hopping between the d orbitals due to the orbital polarization.

there are just two double representations Γ_6 and Γ_7 for the C_{4v} group; we have used primes on Γ_7 to indicate its different orbital character (see Table I) due to the symmetry-allowed mixing between the two Γ_7 states in the t_{2g} manifold [12].

The remaining parts, $V_{\rm sf}$ and $\mathcal{H}_E$, in Eq. (2) are the inversion symmetry breaking fields crucial for the Rashba effect. The surface field $V_{\rm sf}$ is modeled by an asymmetric energy for the surface orbitals: $\varepsilon = \varepsilon(xz/yz) - \varepsilon(xy)$ and $\delta = \varepsilon(z^2) - \varepsilon(x^2 - y^2)$, an asymmetry that may come from strain, the electric field via the atomic relaxation it produces, or the hopping differential between the orbitals, e.g., xy and xz/yz [17], and as such has a complex dependence on the electric field. The electric field part $\mathcal{H}_E$ induces new hoppings (Fig. 5) between atoms: $\alpha = \langle xy|\mathcal{H}_E|xz\rangle_{\hat{y}}$, $\beta = \langle xz|\mathcal{H}_E|z^2\rangle_{\hat{x}}$, and $\gamma = \langle x^2 - y^2|\mathcal{H}_E|yz\rangle_{\hat{y}}$, whose strengths are roughly proportional to the local electric field. Here the subscript denotes the direction of the nearest neighbor on which the second orbital is located. Typical parameters for KTO are [18,19]: $\Delta = \varepsilon(e_g) - \varepsilon(t_{2g}) \approx 4$ eV, $\xi \approx 0.26$ eV, $V_\sigma \approx -1$ eV, $V_\pi \approx -0.5$ eV, while α, β, and γ are $\sim$10 meV at the surface layer. As one goes into the bulk, the inversion symmetry-breaking parameters ϵ, δ, α, β, and γ rapidly go to zero, so that the Rashba effect comes just from the first few surface layers.

We obtain the Rashba splitting from Eq. (2) by Löwdin downfolding [12,20] of the effects of the higher-energy bands. The results can be expressed in the Rashba form $\mathcal{H}_R = \alpha_R(\vec{k} \times \vec{\sigma}) \cdot \hat{z}$ for most bands and the corresponding Rashba coefficients and the partner functions for the pseudospin $\vec{\sigma}$ are listed in Table I. However, for near-degenerate cases, where the SOI is strong ($\xi \gg |\varepsilon|$) but the surface field does not sufficiently lift the fourfold degeneracy of the Γ_8^+ state ($|\varepsilon| \ll |\alpha|$ or $|\varepsilon| \sim |\alpha|$), the Löwdin downfolding fails and the Rashba SOI can only be written as a 4×4 matrix spanning the Γ_8^+ subspace:

$$\mathcal{H} = \frac{2}{3}\begin{pmatrix} ak^2 + \varepsilon & 2\alpha k_+ & c\bar{k}^2 & -\sqrt{3}\alpha k_+ \\ 2\alpha k_- & ak^2 + \varepsilon & \sqrt{3}\alpha k_+ & -c\bar{k}^2 \\ c\bar{k}^2 & \sqrt{3}\alpha k_- & bk^2 & \frac{3\sqrt{3}\beta\xi}{\Delta}k_+ \\ -\sqrt{3}\alpha k_+ & -c\bar{k}^2 & \frac{3\sqrt{3}\beta\xi}{\Delta}k_- & bk^2 \end{pmatrix}. \tag{3}$$

Here, we have included the quadratic-k terms (the band mass), with $k_\pm = k_y \pm ik_x$, $\bar{k}^2 = (k_+^2 - k_-^2)$, $a = -5V_\pi/3$, $b = -V_\pi/2$, and $c = -\sqrt{3}V_\pi/4$, and the order of the basis is the same as the order of appearance of the four Γ_8^+ partner functions in case 2, Table I. The Rashba part $\mathcal{H}_R$ is simply Eq. (3) minus the k^2 terms. Equation (3) is valid for strong ξ and for any ε and α. If $|\varepsilon| \gg |\alpha|$, one recovers the results of case 2, Table I using Löwdin downfolding. Figure 6 shows the TB bands for cases relevant to the Rashba splitting seen in the DFT bands.

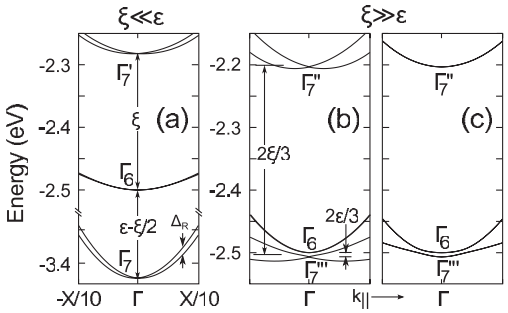

FIG. 6. Rashba splitting of the t_{2g} states in two different regimes of the SOI strength ξ. Panel (a) corresponds to a weak $\xi \ll \varepsilon$ (in eVs, $\xi = 0.2$, $\alpha = 0.05$, $\varepsilon = 1$) (case 1 in Table I). In (b) and (c), since ξ is strong ($\xi \gg \varepsilon$), but the electric field, parametrized by α, is not weak ($\xi = 0.2$, $\alpha = 0.05$, $\varepsilon = 0.01$), the splitting of the near-degenerate fourfold bands must be described by Eq. (3). (c) Shows the same parameters as (b) except $\alpha = 0$, so that there is no Rashba splitting in (c).

Note from Table I that even though the linear-k Rashba splitting is always present, its magnitude is very small ($\sim 1/\Delta$) for the e_g bands as well as for the t_{2g}-derived Γ_6 bands. For these bands, the higher-order k^3 term may in fact be dominant as has been seen in the $SrTiO_3$ surface [21] and also suggested by Zhong *et al.* [22]. Also as Table I shows, the pseudospin partner functions are sometimes not spin entangled at the Γ point (i.e., spin-up and -down states don't mix), but they always become entangled away from Γ due to the spin mixing via the Rashba Hamiltonian. Returning to the t_{2g} bands, which make up the 2DEG, for small SOI ξ relative to the surface field ε (case 1 in the Table), the Rashba coefficient can be small if ε is large [note that $\varepsilon = \varepsilon(xz/yz) - \varepsilon(xy)$ can be varied widely in a material due to lattice relaxation, electric field, or strain, while ξ is more or less fixed]. The Rashba effect is enhanced significantly in the opposite limit ($\xi \gg |\varepsilon|$), if at the same time the surface field ε is small or comparable to the electric-field-induced hopping α. In this scenario, the Rashba effect is described by Eq. (3). This is the case for Figs. 6(b) and (c), where a large Rashba splitting is seen for the Γ_7''' bands, and also for the DFT bands [Figs. 3(a) and (c)]. Thus the electric field changes the Rashba effect in two ways: first, by changing the density of the 2DEG in the surface layers, and second, by altering the surface asymmetry field ε and reorienting the orbital energies.

In conclusion, we showed that the Rashba effect can be tuned in the polar perovskite oxides by manipulating the 2DEG profile by an external electric field. These

results are relevant not just for the KTO surface, but also for polar materials in general that contain surface or interface *d* electrons. We also note that since the energies of the *d* orbitals are sensitive to the applied strain, this suggests another means of tailoring the Rashba effect.

We thank Zoran Popović for stimulating discussions and computational help. This work was supported by the Office of Basic Energy Sciences of the U. S. Department of Energy through Grant No. DE-FG02-00ER45818.

*Corresponding author.
shanavasv@missouri.edu

[1] E. I. Rashba, Sov. Phys. Solid State **2**, 1109 (1960); Y. A. Bychkov and E. I. Rashba, J. Phys. C **17**, 6039 (1984); Y. A. Bychkov and E. I. Rashba, JETP Lett. **39**, 78 (1984).
[2] R. Winkler, *Spin-Orbit Effects in Two-Dimensional Electron and Hole Systems* (Springer, New York, 2003).
[3] J. Nitta, T. Akazaki, H. Takayanagi, and T. Enoki, Phys. Rev. Lett. **78**, 1335 (1997).
[4] A. Ohtomo, D. A. Muller, J. L. Grazul, and H. W. Hwang, Nature (London) **419**, 378 (2002).
[5] A. Ohtomo, and H. W. Hwang, Nature (London) **427**, 423 (2004).
[6] M. Ben Shalom, M. Sachs, D. Rakhmilevitch, A. Palevski, and Y. Dagan, Phys. Rev. Lett. **104**, 126802 (2010).
[7] A. D. Caviglia, M. Gabay, S. Gariglio, N. Reyren, C. Cancellieri, and J.-M. Triscone, Phys. Rev. Lett. **104**, 126803 (2010).
[8] P. D. C. King *et al.*, Phys. Rev. Lett. **108**, 117602 (2012).
[9] A. F. Santander-Syro, C. Bareille, F. Fortuna, O. Copie, M. Gabay, F. Bertran, A. Taleb-Ibrahimi, P. Le Fèvre, G. Herranz, N. Reyren, M. Bibes, A. Barthélémy, P. Lecoeur, J. Guevara, and M. J. Rozenberg, Phys. Rev. B **86**, 121107 (2012).
[10] G. Kresse and J. Hafner, Phys. Rev. B **47**, 558 (1993).
[11] G. Kresse and J. Furthmuller, Phys. Rev. B **54**, 11169 (1996).
[12] See Supplemental Material at http://link.aps.org/supplemental/10.1103/PhysRevLett.112.086802 for the tight-binding derivation of the Rashba effect as well as for details of the symmetry representations, the density-functional methods used in our calculations, surface relaxation, as well as for some results for the KO-terminated surface.
[13] G. Bihlmayer, Yu. M. Koroteev, P. M. Echenique, E. V. Chulkov, and S. Blügel, Surf. Sci. **600**, 3888 (2006).
[14] S.-J. Gong, C.-G. Duan, Y. Zhu, Z.-Q. Zhu, and J.-H. Chu, Phys. Rev. B **87**, 035403 (2013).
[15] L. Petersen and P. Hedagard, Surf. Sci. **459**, 49 (2000).
[16] G. F. Koster, J. O. Dimmock, R. G. Wheeler, and H. Statz, *Properties of the Thirty-Two Point Groups* (MIT Press, Cambridge, MA, 1963).
[17] Z. S. Popović, S. Satpathy, and R. M. Martin, Phys. Rev. Lett. **101**, 256801 (2008).
[18] G. E. Jellison, I. Paulauskas, L. A. Boatner, and D. J. Singh, Phys. Rev. B **74**, 155130 (2006).
[19] T. Neumann, G. Borstel, C. Scharfschwerdt, and M. Neumann, Phys. Rev. B **46**, 10623 (1992).
[20] P. Löwdin, J. Chem. Phys. **19**, 1396 (1951).
[21] H. Nakamura, T. Koga, and T. Kimura, Phys. Rev. Lett. **108**, 206601 (2012).
[22] Z. Zhong, A. Tóth, and K. Held, Phys. Rev. B **87**, 161102 (2013).